

Influence of molybdenum oxide on structural, optical and physical properties of oxychloride glasses for nonlinear optical devices

F. Goumeidane, M. Iezid, B. Melik, K. Ouannes, M. Legouera, M. Poulain, T. Satyanarayana, P.S. Prasad, P.V. Rao

▶ **To cite this version:**

F. Goumeidane, M. Iezid, B. Melik, K. Ouannes, M. Legouera, et al.. Influence of molybdenum oxide on structural, optical and physical properties of oxychloride glasses for nonlinear optical devices. Ceramics International, 2017, 43 (14), pp.11305-11311. 10.1016/j.ceramint.2017.05.329 . hal-01581243

HAL Id: hal-01581243

https://univ-rennes.hal.science/hal-01581243

Submitted on 4 Sep 2017

HAL is a multi-disciplinary open access archive for the deposit and dissemination of scientific research documents, whether they are published or not. The documents may come from teaching and research institutions in France or abroad, or from public or private research centers.

L'archive ouverte pluridisciplinaire **HAL**, est destinée au dépôt et à la diffusion de documents scientifiques de niveau recherche, publiés ou non, émanant des établissements d'enseignement et de recherche français ou étrangers, des laboratoires publics ou privés.

ACCEPTED MANUSCRIPT

Influence of molybdenum oxide on structural, optical and physical properties of oxychloride glasses for nonlinear optical devices

Goumeidane F[a], Iezid M[a], Melik B[a], Ouannes K[b], Legouera M[c], Poulain M[d], T. Satyanarayana[e], P. Syam Prasad[f], P. Venkateswara Rao[g*]

[a]Laboratoire de Génie Mécanique, université de Biskra, BP 145, Biskra, Algeria

[b]Faculté des Sciences et de la Technologie, Université de Biskra, BP 145, Biskra, Algeria

[c]Laboratoire de Génie Mécanique et Matériaux, Université de Skikda, 21000, Algeria

[d]Institut Sciences Chimiques, Université de Rennes1, Campus Beaulieu, F-35042 Rennes

[e]Dept. of Electronics & Instrumentation Engineering, Lakireddy Bali Reddy College of Engineering (A), Mylavaram, Krishna 521230, A.P., India

[f]Dept. of Physics, National Institute of Technology (NIT), Warangal-506 004, Telangana State, India

[g]Department of Physics, The University of the West Indies, Mona Campus, Kingston 7, Jamaica

[*]Corresponding author : pvrao54@gmail.com

Accepted manuscript

Abstract

The unconventional Heavy Metal Oxide Glasses (HMOG) are characterized by a low phonon energy, large infrared range transmission, high refractive index and nonlinear optical properties. Ternary glasses have been synthesized and studied in the Sb_2O_3–MoO_3-$ZnCl_2$ system. Further, the glass formation compositional limits are reported and some glass samples with the formula: (90-x)Sb_2O_3 -xMoO_3–10 $ZnCl_2$ ($10 \leq x \leq 50$, mole %) were elaborated. Thermal properties have been measured and indicating that the glass transition temperature decreases with increasing proportions of molybdenum oxide. The evolution of density, microhardness and elastic modulus has been studied as functions of parameter x and Raman spectra measurements have been shown the partial conversion of MoO_6 octahedral units into MoO_4 tetrahedral.

Keywords: Oxychloride glasses; Density; Raman, Elastic properties; Optical properties

1. Introduction

ACCEPTED MANUSCRIPT

Over the past few years, several researches have been carried out on antimony glasses. Binary and ternary Sb_2O_3-based glasses have been studied, including various oxide [1-6], oxysulphide [7, 8] and oxychloride systems [9, 10]. These glasses are used in nonlinear optical devices particularly in broadband optical amplifiers functioning about 1.5μm [11].

Molybdenum oxide is considered as a glass former that requires the presence of other elements to form a glass. Molybdate glasses are obtained by introducing another network-forming oxide such as Sb_2O_3, P_2O_5, TeO_2 …etc. The molybdate glasses are used for high-density memories, light modulation, large area display devices like smart windows and other electrochromic systems [12,31,32]. The different oxidation states of molybdenum are: Mo^{6+}, Mo^{5+}, Mo^{4+} and Mo^{3+}. In the molybdate glasses, different works suggest the existence of molybdenum in the Mo^{6+} form which is the most stable [13]. Rada et al [14] suggest that a part of the Mo^{6+} ions is converted into Mo^{3+} and Mo^{5+} ions . This process causes the depolymerisation of host glass network. The molybdenum oxide is formed in the glass by different structures, like structural units of octahedron and tetrahedron units such as MoO_6 and MoO_4 respectively. Krapchanska et al [15] showed a partial conversion of MoO_6 to MoO_4 units in the MoO_3-TiO_2-Bi_2O_3 system. Subcik et al [16] also showed that the incorporation of MoO_3 units in the ZnO-B_2O_3- P_2O_5 glasses revealed the increase of the MoO_6/ MoO_4 ratio.

Sb_2O_3 contributes in the glass network with SbO_3 structural units and it appears tetrahedra with the oxygens to be found at three corners and the lone pair of electrons of antimony Sb^{3+} at the fourth corner localized in the third equatorial direction of the Sb atom. There may be a possibility of existence of antimony ions in the Sb^{5+} state and participate in the glass network forming with $Sb^{5+}O_4$ structural units may enhance the nonlinear optical properties [11]. In Sb_2O_3 based glasses the addition of transition metal

Accepted manuscript

ACCEPTED MANUSCRIPT

oxide MoO_3 improves functionality of glasses for their desired optical applications. Particularly, MoO_3 shows interesting optoelectronic features and can control phase separation in glasses [43].

The aim of this paper is focuses on the elaboration of a new antimony oxychloride glass from the Sb_2O_3-MoO_3- $ZnCl_2$ system. We are interested by molybdenum rates incorporated into the glass, its effect on the different physical properties that have been measured, and especially in the structural study by Raman measurements. Physical properties such as: density, energy dispersive spectroscopy (EDS), differential scanning calorimetry (DSC), optical transmission, microhardness and elastic moduli have also been considered in terms of molybdenum influence.

2. Experimental

In this present study, the starting materials Sb_2O_3≥99% (Acros), $ZnCl_2$ ≥99.8% (Merck) and MoO_3≈ 99% (Acros) are used for the synthesis of the glass samples. Melt-quenching is the process of synthesis. The powders are mixed thoroughly in a mortar with the mean batch weight around 5 g. The mixture is inserted into a silica glass tube, about 10 mm in diameter and then subjected to a flame until a clear liquid obtaining. The bath of fusion is cast in a mould under preheated brass plate around 200 °C. The samples obtained (thickness of a few millimetres) are placed in the furnace at a temperature lower than the temperature of vitreous transition with a slow heating rate. After annealing, the samples were polished for physical measurements.

The glass composition was analyzed by the (EDS) energy dispersive spectroscopy (JSM 6400 Jeol and Oxford link ISIS). With the help of crystalline materials references, experimental error is estimated to be 1% for Sb, Mo and Zn, 2%

Accepted manuscript

ACCEPTED MANUSCRIPT

for Cl and 5% of oxygen. Density was determined using a helium pycnometer (Micromeritics, AccuPyc 1330) with ±0.001 g/cm^3 accuracy.

Thermal properties of the samples were measured by the differential scanning calorimetry (DSC 2010 from TA Instruments) at the heating rate of 10 K/min with the sensitivity better than 0.1 ^{0}C. The estimated accuracy is ±2 K for the glass transition temperature Tg, crystallization temperature Tx and ± 1 K for the temperature of the crystallization of peak. Tx-Tg provides the stability against devitrification. The DSC signals showed no crystallization peaks indicating that these glasses are having a very low tendency to crystallization and exhibiting extremely high thermal stability. Thermal stability is the important property of glasses and gives the measure of the degree of disorder of glassy state.

The analysis of the vitreous samples was carried out by the Raman spectroscopy in the range of 1100 cm^{-1} to 100 cm^{-1} by Sentra- Bruker. Varian Cary 5 spectrometer was used to record the optical transmission in the UV–visible spectrum between 400 and 800 nm and Bomem Michelson 100 IR spectrometer was employed for the infrared spectrum in between 500 and 4000 cm^{-1}.

The Matzuzawa MXT 70 digital microhardness was used with 100 g as load to measure the microhardness values. Ultrasonic measurements were taken by the pulse – echo method using a Panametrics model 5800 pulser/receiver with a quartz transducer. Both X-cut transducer and Y-cut transducer (with 10 MHz frequency) were employed for both longitudinal and shear modes. A Hewlett-Packard model 54502A oscilloscope recorded the pulse transient. Young's modulus E, bulk modulus K, and shear modulus G were measured by the following equations [33]:

Accepted manuscript

ACCEPTED MANUSCRIPT

$$E = \frac{\rho V_T^{\,2}\left(3V_L^{\,2} - 4V_T^{\,2}\right)}{\left(V_L^{\,2} - V_T^{\,2}\right)} \quad (1)$$

$$K = \frac{\rho\left(3V_L^{\,2} - 4V_T^{\,2}\right)}{3} \quad (2)$$

$$G = \rho V_T^{\,2} \quad (3)$$

Where ρ = Density of the glass sample

V_T = Transversal ultrasonic velocity

V_L = Longitudinal ultrasonic velocity

The uncertainty is estimated to be about ± 2% for elastic modulus.

3. Results and discussion

3.1. Physical properties

Chemical composition, some experimental properties of SMZ glasses are provided in Table 1. Fig. 1 shows the Oxy-halogenated glass area for ternary system. The glass matrix Sb_2O_3 -MoO_3- $ZnCl_2$ was characterized by its extensive glass area and exceptional thermal stability. We have chosen to vary the molybdenum oxide, which is an excellent effect in heating homogenization [17, 18]. It is used for its electrochromic properties [19] and especially for improving the conductivity by the ionic and electronic input [20, 21]. A series of ternary system bulk samples were prepared for the physical measurements and were represented by the lines in Fig. 1 with the formula: (90-x) Sb_2O_3-xMoO_3-10$ZnCl_2$ (10≤x≤50) called «SMZ». The molar concentration of MoO_3 is given by the number that follow the letters SMZ.

Glass compositions of the prepared samples were studied by the EDS spectra. Fig.2 shows the chemical composition spectra of the sample SMZ20. In Table 1 it is clear from the chemical composition of the glasses that the differences between the

Accepted manuscript

ACCEPTED MANUSCRIPT

nominal and analysed cations compositions remain weak. These results indicate that the losses induced by evaporation during fusion are very limited. Silicon traces lower than 1% are observed in all the samples, due to crucible contamination. The measurement of concentration refers to the three analysed elements. Discrepancies are larger for anions; this can be explained by the limited accuracy of the EDS technique for light elements, particularly for the oxygen. Uncertainty related to electronic scan microscopy results is about 1%.

The density and molar volume of the glass samples decreases linearly with the substitution of the antimony oxide and molybdenum oxide. The density of a solid glass is a function of its composition; in fact, it is directly depends on the atomic weight of each component as well as the volume occupied by these components [22]. This reduction is due to the lower atomic weight of the molybdenum than the antimony.

Accepted manuscript

3.2. Thermal properties

DSC curves for different glasses are shown in Fig. 4. The characteristic temperatures of the glass samples have been measured for the glass series (90-x)Sb_2O_3-xMoO_3- 10$ZnCl_2$. The thermal stability Tx-Tg, exceeds 100 °C for all the glass samples (Table 2). The numerical values obtained from the DSC curves provides the information on stability against devitrification (20 K/min). As shown in Table 2, from the results of DSC, when the concentration of MoO_3 increases from 10 to 50 %, the glass transition temperature decreases linearly (Fig. 5), indicates the decreasing bonding strength of the material. Goumeidane et al. [10] was mentioned that an excess of anionic oxygen which causes the increase of the nonbridging oxygen in the vitreous network. This conclusion could explain the decreased values of transition temperature Tg in the glass system.

ACCEPTED MANUSCRIPT

3.3. Optical properties

In the infrared spectrum, the glasses can transmit up to 1800 cm^{-1} (Fig. 6). The spectrum shows a large absorption band around 3300 cm^{-1}, originates from OH groups. A second extrinsic absorption band is observed between 1700 and 1900 cm^{-1}, which limits the effects of the optical transmission of these glasses. It corresponds to the first harmonic of the fundamental of Si-O vibration band at 1984 cm^{-1} and arises probably from silicate anions from glass crucibles. The multiphonon absorption cannot be identified accurately under these conditions. Generally, due to low phonon energy of the oxyfluoride or oxychloride glasses, when rare earth ions are doped into them, the multiphonon relaxation rates are reduced from emitting levels to lower states, which causes the quantum efficiencies to increase for various photonic applications[44,45]. UV-visible depends on the energy band gap between the valence and conduction electronic layers of material. It has been determined by the Urbach method. The UV–visible spectrum for $50Sb_2O_3$- $40MoO_3$-10 $ZnCl_2$ glass sample (2.5 mm in thickness) has been shown in Fig. 7 and the UV–visible transmission edge was around 516 nm. Fig. (7) shows the Urbach plot of $50Sb_2O_3$- $40MoO_3$-10 $ZnCl_2$ glass sample. The value of optical band gap obtained from the extrapolation of the curve is 2.39 eV.

3.4. Raman spectra

The Raman spectra (Fig. 8) of the ternary system's vitreous samples are recorded at ambient temperature in the spectral range 1500 – 50 cm^{-1}. The broad peaks and Boson peak confirm the glassy state below 100 cm^{-1}, which is ubiquitous in the Raman spectra of disordered solids, especially of glasses. The presence of the Boson peak in the Raman spectra affirms the vitreous state of material [6] which has not an equivalent in the crystalline materials. The Raman spectra of SMZ 10 glasses reveal the

Accepted manuscript

ACCEPTED MANUSCRIPT

presence of the band at 416 cm^{-1}, related to symmetric stretching vibrations of the pyramids SbO_3 and ZnO_4 units. This band intensity decreases with the increase of MoO_3 from 10% to 30%. We recorded a small shift in the SMZ 20 and SMZ 30 samples, associated with the same vibration mode, they are toward 424 cm^{-1} and 413 cm^{-1} respectively. Moreover, the shoulder at 183- 205 cm^{-1} is assigned to the vibration of ZnO_6 units.

In previous papers [34–42], it has been established that MoOn polyhedral like MoO_4 tetrahedral units and MoO_6 octahedra units gave strong Raman bands. In the region 700–1000 cm^{-1}, Raman bands corresponding to symmetric stretching modes (υ_1) and asymmetric stretching modes (υ_3) are observed. Yet, Raman bands attributed to symmetric bending modes (ν_2) and asymmetric bending modes (ν_4) are noticed in the wavenumber range of 300–520 cm^{-1} [26]. In figure 8, the spectra's peak position of glasses containing molybdate oxide indicates that the strong band at 918-936 cm^{-1} could be attributed to the deformed vibrational mode of MoO_6 [24]. Beyond of 20% of MoO_3, a partial conversion of MoO_6 units to MoO_4 units. This transformation is assisted by Zn^{+2} or Zn^{+3} [23]. We noticed that the intensity of MoO_6 increases, whereas the band of SbO_3, ZnO_4 decreases may be the presence of $Mo^{5+}O_3^-$ complexes in the structural network of the glass series and generates the depolymerisation of zinc and /or antimonite chains in the vitreous samples [24]. Additionally, the ν_1 and ν_2 vibrational bands of monomeric MoO_4^{2-} tetrahedral units have also been located at about 862-869 cm^{-1} and 327-346 cm^{-1} respectively.

For the ZnO-B_2O_3-MoO_3 system, Alexandrov et al [25] deconvolution of the Raman spectrum in the regions 600- 1100 cm^{-1} into 6 peaks with positions at: 830, 880, 920 and 950 cm^{-1}, showing the presence of Mo^{6+} ions in MoO_4^{2-} with more coordination, one peak at 780 cm^{-1} with isolated MoO_4 units, and the last band corresponds to the

Accepted manuscript

ACCEPTED MANUSCRIPT

stretching vibration of BO_4 at 1000-1200 cm^{-1}. In our case, the spectra are fitted with a sum of Gaussian curves by means of the least square method as shown in Fig. 9, the deconvolution is performed in the same interval. We found three peaks at 780 cm^{-1} assigned to isolated MoO_4 units, 860 cm^{-1} and 920 cm^{-1} indicate that Mo^{6+} ions are present in $(MoO4)^{2-}$ tetrahedral units for the glass sample SMZ20. The analysis of the spectra of SMZ30, SMZ40 and SMZ50 glasses shows the appearance of a new peak at 820 cm^{-1} in addition to the previous ones (780, 860 and 920 cm^{-1}). Probably, this shows a structural change at 20% of molybdenum with the formation of Mo^{6+} ions in different coordination's, namely low symmetry, highly distorted, or isolated in MoO_4^{2-} [26].

Finally, we notice that the Zinc chloride is involved in the vitreous network by $ZnCl_4^{-2}$ tetrahedra and as shown by the Raman analysis, zinc chloride portion becomes an oxide. The peaks at 233 and 275 cm^{-1} are assigned to the symmetric Zn–Cl stretching vibrations in type A and B respectively [27]. The peaks are not resolved in this work because of the small amount of zinc chloride in the series of glasses and the intrinsic peak broadening of the Raman spectrum corresponding to the state of an amorphous solid (glassy state).

3.5. Microhardness

Microhardness (H_V) was measured for all the samples, as shown in Fig. 10 the state of the microhardness curve is adjusted by the expansion of the MoO_3 content. The evaluation is monotonic for the MoO_3/Sb_2O_3 substitution, it drops from 229 to 172 N/mm^2 between 10 and 50 mol %. This evolution was explained by the variation of the bond strength and also the dissociation energy. The microhardness of the samples increases with the molybdenum content in the glasses, corresponding to a consolidation of the glass by an increasing of the Mo-O strength bonds. Furthermore, the

Accepted manuscript

ACCEPTED MANUSCRIPT

molybdenum enters in the glass network as a glass former and contributes to the formation of rigid structural units as well as strengthening the rigidity of the glass structure.

3.6. Elastic properties

Elastic moduli E, G, K have been calculated for the SMZ glass series. A general observation of these curves shows (Fig.11) that elastic moduli increase with the substitution of Sb_2O_3 by MoO_3. There are several models for the interpretation of elastic moduli of oxide glasses. In literature, few studies referred to elastic moduli of oxychloride based antimonite Iezid et al. [9]. The series of glasses comprises 90% of the oxides and 10% of $ZnCl_2$. This chloride has a low binding energy compared to oxides and we assume that the $ZnCl_2$ effect on the elastic modulus is negligible. So, elastic moduli of oxide glasses apply in a good approximation in our case. The model of Mackashima and Mackanzi [28, 29] explains the Young's modulus by increasing the dissociation energy and the packing density factor following the increase in the content of MoO_3.

The limited variation of shear modulus can be explained by the model of Bridge B et al [30]. We assume that the cross-link densities are run by an almost constant recovery among bridging oxygen and nonbridging, which limits the variation of G.

The evaluation of K can be explained by the Bulk compression model [30] in the sense that the insertion of MoO_3 increases the stretching bond strength since the dissociation energy of M-O is greater than Sb-O.

4. Conclusion

Accepted manuscript

ACCEPTED MANUSCRIPT

A ternary glass system is synthesised and the broad vitreous area is observed in the Sb_2O_3 -MoO_3- $ZnCl_2$ system. A glass samples in which Sb_2O_3 is substituted by MoO_3 have been characterized. The differential scanning calorimetry analysis shows that all the compositions have a large thermal stability (Tx-Tg > 100 °C). The IR transmission is spread out from the visible to infrared due to the low phonon energy of the antimonite. The general trend is that MoO_3 incorporation leads to the decrease of density from 5.038 to 4.722 g/cm^3, glass transition temperature T_g from 279 to 259 °C whereas the microhardness (172 to 229 N/mm^2) and the rigidity (elastic moduli) increases. The Raman spectroscopy provides the partial conversion of molybdenum ions from MoO_6 octahedral to MoO_4 tetrahedral positions from 20% of MoO_3. The quality of these high stability glasses makes them a potential application for optoelectronic devices.

Acknowledgements

The support of the Authorities of the Laboratoire de Génie Mécanique, université de Biskra, Algeria, the Principal's New Initiative grant by the university of the West Indies, Mona campus, Jamaica and Lakireddy Bali Reddy College of Engineering (A), Mylavaram, A.P., India is highly acknowledged.

Accepted manuscript

References

[1] M. Soltani, T. Djouama, A. Boutarfaia, M. Poulain, New heavy metal oxide glasses based on Sb_2O_3, J. Optoelectron. Adv. Mater. Symp.1 (2009) 339-342.
[2] M. Nalin, M. Poulain, M. Poulain, S.J. Ribeiro, Y. Messaddeq, Antimony oxide based glasses, J. Non-Cryst. Solids. 284 (2001) 110-116.

ACCEPTED MANUSCRIPT

[3] M. Hamzaoui, M. Soltani, M. Baazouzi, B. Tioua, Z. Ivanova, R. Lebullenger, M. Poulain, J. Zavadil, Optical properties of erbium doped antimony based glasses: Promising visible and infrared amplifiers materials, phys. status solidi (b). 249 (2012) 2213-2221.

[4] M. Kubliha, M. Soltani, V. Trnovcová, M. Legouera, V. Labaš, P. Kostka, D. Le Coq, M. Hamzaoui, Electrical, dielectric, and optical properties of Sb_2O_3-Li_2O- MoO_3 glasses, J. Non-Cryst. Solids. 428 (2015) 42-48.

[5] M. Soltani, M. Hamzaoui, S. Houhou, H. Touiri, L. Bediar, A. Ghemri, P. Petkova, Physical Characterization of Sb_2O_3-M_2O-MoO_3 (M= Li, K) New Glasses, Acta Phys. Pol. A 123 (2013) 227-229.

[6] K. Ouannes, K. Lebbou, Brian-M. Walsh, M. Poulain, G. Alombert-Goget, Y. Guyot, New Er^{3+} doped antimony oxide based glasses: Thermal analysis, structural and spectral properties, J. Alloys Compd. 649 (2015) 564-572.

[7] L. Zan, J. Zhong, Q. Luo, New oxysulphide glasses from the Sb_2O_3-Sb_2S_3.M_xS system, J. Non-Cryst. Solids. 257 (1999) 396-399.

[8] R. Makhloufi, A. Boutarfaia, M. Poulain, New oxysulphide glasses in Sb_2S_3– M_mO_n and Sb_2S_3– Sb_2O_3–M_mO_n systems, J. Alloys Compd. 398 (2005) 249-255.

[9] M. Iezid, M. Legouera, F. Goumeidane, M. Poulain, V. Nazabal, R. Lebullenger, Glass formation in the Sb_2O_3-$CdCl_2$-$SrCl_2$ ternary system, J. Non-Cryst. Solids. 357 (2011) 2984-2988.

[10] F. Goumeidane, M. Legouera, M. Iezid, M. Poulain, V. Nazabal, R. Lebullenger, Synthesis and physical properties of glasses in the Sb_2O_3-$PbCl_2$-MoO_3 system, J. Non-Cryst. Solids. 357 (2011) 3572-3577.

[11] V. Himamaheswara Rao, P. Syam Prasad, P. Venkateswara Rao, L.F. Santos, N.Veeraiah, Influence of Sb_2O_3 on tellurite based glasses for photonic applications, J. Alloys Compd. 687 (2016) 898–905.

[12] P. Srinivasa Rao, P.M. Vinaya Teja, A. Ramesh Babu, Ch. Rajyasree, D. Krishna Rao, Influence of molybdenum ions on spectroscopic and dielectric properties of ZnF_2-Bi_2O_3-P_2O_5 glass ceramics, J. Non-Cryst. Solids. 358 (2012) 3372-3381.

[13] R.J. Short, R.J. Hand, N.C. Hyatt, An Investigation into the Oxidation State of Molybdenum in Simplified High Level Nuclear Waste Glass Compositions, Mater. Res. Soc. Symp. Proc. 757 (2003) 141–146.

[14] S. Rada, E. Culea, R. Chelcea, M. Rada, A. Bot, N. Aldea, V. Rednic, Physical properties and electrochemical performance of molybdenum–lead-germanate glasses and glass ceramics, Ceram. Int. 39 (2013) 1403-1411.

[15] M. Krapchanska, R. Iordanova, Y. Dimitriev, A. Bachvarova-Nedelcheva, Glass formation in the system MoO_3-TiO_2- Bi_2O_3, J. Optoelectron. Adv. Mater. 12 (2010) 1692-1695.

[16] J. Šubčík, L. Koudelka, P. Mošner, L. Montagne, B. Revel, I. Gregora, Structure and properties of MoO_3-containing zinc borophosphate glasses, J. Non-Cryst. Solids. 355 (2009) 970-975.

[17] G. Poirier, C.B. de Araujo, Y. Messaddeq, S.J. Ribeiro, M. Poulain, Tungstate fluorophosphate glasses as optical limiters, J. appl. phys.91 (2002) 10221-10223.

[18] B. Bridge, N. Patel, The elastic constants and structure of the vitreous system Mo-PO, J. mater sci. 21 (1986) 1187-1205.

[19] B. Chowdari, P.P. Kumari, Studies on Ag_2OMxOy.TeO_2 (MxOy=WO_3, MoO_3, P_2O_5 and B_2O_3) ionic conducting glasses, Solid State Ionics. 113(1998) 665-675.

[20] J. Yao, Y. Yang, B. Loo, Enhancement of photochromism and electrochromism in MoO_3/Au and MoO_3/Pt thin films, J.Phys. Chem. B. 102 (1998) 1856-1860.

Accepted manuscript

ACCEPTED MANUSCRIPT

[21] R. Berger, P. Beziade, A. Levasseur, Y. Servant, Electron spin resonance of vitreous lithium boromolybdates, Phy. chem. Glasses. 31 (1990) 231-238.
[22] M. Volf, Mathematical approach to glass. 1988, Amsterdam, Elsevier.
[23] M. Milanova, R. Iordanova, L. Aleksandrov, M. Hassan, Y. Dimitriev, Glass formation and structure of glasses in the ZnO-Bi_2O_3-WO_3-MoO_3 system, J. Non- Cryst. Solids. 357 (2011) 2713-2718.
[24] S.B.M. Krishna, A.R. Babu, RSree. Ch, D.Krishna Rao, Influence of molybdenum ions on the structure of ZnO–As_2O_3–Sb_2O_3 glass system by means of spectroscopic and dielectric studies, J. Non-Cryst. Solids. 356 (2010) 1754-1761.
[25] L. Aleksandrov, T. Komatsu, R. Iordanova, Y. Dimitriev, Study of molybdenum coordination state and crystallization behavior in MoO_3-La_2O_3-B_2O_3 glasses by Raman spectroscopy, J. Phys. Chem. Solids. 72 (2011) 263-268.
[26] L. Aleksandrov, T. Komatsu, R. Iordanova, Y. Dimitriev, Structure study of MoO_3-ZnO-B_2O_3 glasses by Raman spectroscopy and formation of α-$ZnMoO_4$ nanocrystals, Opt. Mater. 33 (2011) 839-845.
[27] K. Kinugawa, K. Kadono, H. Tanaka, Raman spectroscopic study on the structure of $ZnCl_2$-ZnX_2 and $ZnCl_2$-KX (X= Br, I) glasses, J. Non-Cryst. Solids. 110 (1989) 265-272.
[28] A. Makishima, J. Mackenzie, Direct calculation of Young's modulus of glass, J. Non-Cryst. Solids. 12 (1973) 35-45.
[29] A. Makishima, J.D. Mackenzie, Calculation of bulk modulus, shear modulus and Poisson's ratio of glass, J. Non-Cryst. Solids. 17 (1975) 147-157.
[30] B. Bridge, A. Higazy, A model of the compositional dependence of the elastic moduli of polycomponent oxide glasses, Phys. chem. Glasses. 27 (1986) 1-14.
[31] Mogus-Milankovic, A., A. Santic, M. Karabulut, and D. E. Day. Study of electrical properties of MoO_3-Fe_2O_3-P_2O_5 and SrO-Fe_2O_3-P_2O_5 glasses by impedance spectroscopy, J. Non-Cryst. Solids. 330 (2003) 128-141.
[32] L. Bih, M. El Omari, JM. Reau, M. Haddad, D. Boudlich, A. Yacoubi, A. Nadiri, Electronic and ionic conductivity of glasses inside the Li_2O-MoO_3-P_2O_5 system, Solid State Ionics. 132 (2000)71– 85.
[33] A. Delben, Y. Messaddeq, M.D. Caridade and M.A. Aegerter, Mechanical properties of ZBLAN glasses, J. Non-Cryst. Solids. 161 (1993)165-168.
[34] T. Sekiya, N. Mochida, S. Ogawa, Structural study of MoO_3TeO_2 glasses, J. Non-Cryst. Solids. 185 (1995) 135-144.
[35] M. Abe, Y. Benino, T. Fujiwara, T. Komatsu, R. Sato, Writing of nonlinear optical $Sm_2(MoO_4)_3$ crystal lines at the surface of glass by samarium atom heat processing, J. Appl. Phys. 97 (2005) 123516-7.
[36] P. Becker, L. Bohaty, H.J. Eichler, J. Hanuza, A.A. Kaminskii, Observation of many-phonon stimulated Raman scattering and related cascaded nonlinear-laser effects in monoclinic $LaBO_2MoO_4$ single crystals, Laser Phys. Lett. 5 (2008) 114-121.
[37] L. Seguin, M. Figarz, R. Cavagnat, J.C. Lassegues, Infrared and Raman spectra of MoO_3 molybdenum trioxides and $MoO_3.xH_2O$ molybdenum trioxide hydrates, Spectrochim. Acta A 51 (1995) 1323-1344.
[38] J. Hanuza, M. Maczka, K. Hermanowicz, P.J. Deren, W. Strek, L. Folcik, H. Drulis, Spectroscopic properties and magnetic phase transitions in Scheelite $MICr(MoO_4)_2$ and Wolframite $MICr(WO_4)_2$ crystals, where MI= Li, Na, K, and Cs, J. Solid State Chem. 148 (1999) 468-478.

Accepted Manuscript

ACCEPTED MANUSCRIPT

[39] T.T. Basiev, A.A. Sobol, Yu.K. Voronko, P.G. Zverev, Spontaneous Raman spectroscopy of tungstate and molybdate crystals for Raman lasers, Opt. Mater. 15 (2000) 205-216.
[40] G.D. Saraiva, W. Paraguassu, M. Maczka, P.T.C. Freire, J.A. Lima Jr, C.W.A .Paschoal, J.M. Filho, A.G.S. Filho, Temperature-dependent Raman scattering studies of Na_2MoO_4, J. Raman Spectrosc. 39 (2008) 937-941.
[41] J. Hanuza, M. Maczka, J. Lorenc, A.A. Kaminskii, L. Bohaty, P. Becker, Polarised IR and Raman spectra of non-centrosymmetric $Na_3Li(MoO_4)_2 \cdot 6H_2O$ crystal—a new Raman laser material,J. Raman Spectrosc. 41 (2010) 424-430.
[42] C. Luz-Lima, G.D. Saraiva, A.G.Souza Filho, W. Paraguassu, P.T.C. Freire, J.Mendes Filho, Raman spectroscopy study of $Na_2MoO_4 \cdot 2H_2O$ and Na_2MoO_4 under hydrostatic pressure, J. Raman Spectrosc. 41 (2010) 576-581.
[43] G. Lakshminarayana, K.M. Kaky, S.O. Baki, A. Lira, P. Nayar, I.V. Kityk, M.A. Mahdi, Physical, structural, thermal, and optical spectroscopy studies of TeO_2-B_2O_3-MoO_3-ZnO-R_2O (R = Li, Na, and K)/MO (M = Mg, Ca, and Pb) glasses, Journal of Alloys and Compounds (2016), doi: 10.1016/j.jallcom.2016.08.180.
[44] G. Lakshminarayana, E.M.Weis, A.C. Lira, U. Caldiño, D.J.Williams, M.P.Hehlen, Cross Relaxation in Rare-Earth-Doped Oxyfluoride Glasses, J. Lumin. 139 (2013) 132-142.
[45] W. A. Pisarski , J. Pisarska, R. Lisiecki, ł. Grobelny, G. D.-Dzik, W. R.-Romanowski, Luminescence spectroscopy of rare earth-doped oxychloride lead borate glasses, J. Lumin. 131 (2011) 649-652.

Accepted manuscript

Fig. 1. Glass formation in the Sb_2O_3 -MoO_3- $ZnCl_2$ system.

Fig. 2. EDS spectra of glass sample SMZ20 oxychloride glass.

Fig. 3. DSC curves for the SMZ glasses (heating rate 20 K/min).

Fig. 4. Evolution of glass transition temperature versus molybdenum oxide concentration in the (90-x)Sb_2O_3-xMoO_3-10$ZnCl_2$ system.

Fig. 5. Infrared transmission of a 50Sb_2O_3- 40MoO_3-10 $ZnCl_2$ glass sample, 2.5 mm in thickness.

Fig. 6. UV-Visible transmission of a 50Sb_2O_3- 40MoO_3-10 $ZnCl_2$ glass sample, 2.5 mm in thickness.
Fig.7. Urbach plot of 50Sb_2O_3- 40MoO_3-10 $ZnCl_2$ glass sample.

Fig. 8. Raman spectra of SMZ glasses.

ACCEPTED MANUSCRIPT

Fig. 9. Peak deconvolution of Raman spectra of (90-x) Sb_2O_3-xMoO_3-10 $ZnCl_2$ (x=20,30,40 and 50) glasses.

Fig. 10. Microhardness versus composition parameter x for SMZ glasses.

Fig. 11. Evolution of elastic moduli versus composition parameter x for SMZ glasses. E is Young's modulus, K is bulk modulus and G shear modulus.

Table 1. Composition and some experimental properties of SMZ glasses.

Glass	Nominal composition					Analyzed composition						Hv N/mm^2	ρ g/cm^3	V_m cm^3/mol
	Cation %			Anion %		Cation%				Anion%				
	Sb	Zn	Mo	O	Cl	Sb	Zn	Mo	Si	O	Cl			
SMZ 10	88.9	5.55	5.55	93.1	6.9	86.55	6.42	6.63	0.4	79.5	20.5	172	5.038	11.031
SMZ 20	82.35	5.88	11.77	93.1	6.9	82.65	5.1	11.63	0.6	85.09	14.91	194	4.97	10.78
SMZ 30	75	6.25	18.75	93.1	6.9	72.34	6.83	19.73	1.1	92.01	7.99	206	4.892	10.48
SMZ 40	66.66	6.67	26.27	93.1	6.9	58.95	6.8	33.75	0.5	84.86	15.14	223	4.814	10.2
SMZ 50	57.15	7.14	35.71	93.1	6.9	55.87	8	35.43	0.7	95.56	4.44	229	4.722	9.96

Table 2. Characteristic temperatures (°C) and thermal stability range of SMZ glasses: Tg for glass transition, Tx for onset of crystallization and Tp for exothermic maximum.

Glass	Sb_2O_3	MoO_3	$ZnCl_2$	Tg	Tx	Tp	Tx-Tg
SMZ 10	80	10	10	279	401	426	122
SMZ 20	70	20	10	277	412	447	135
SMZ 30	60	30	10	274	466	479	192
SMZ 40	50	40	10	270	405	434	135
SMZ 50	40	50	10	259	376	402	117

Accepted manuscript

ACCEPTED MANUSCRIPT

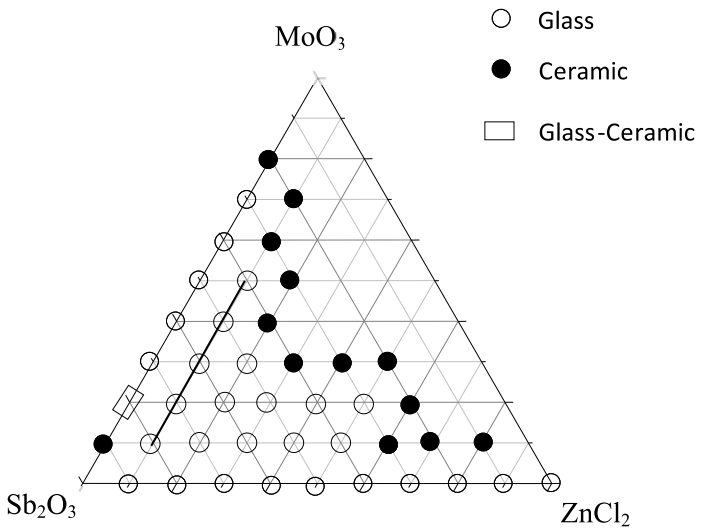


Figure 1

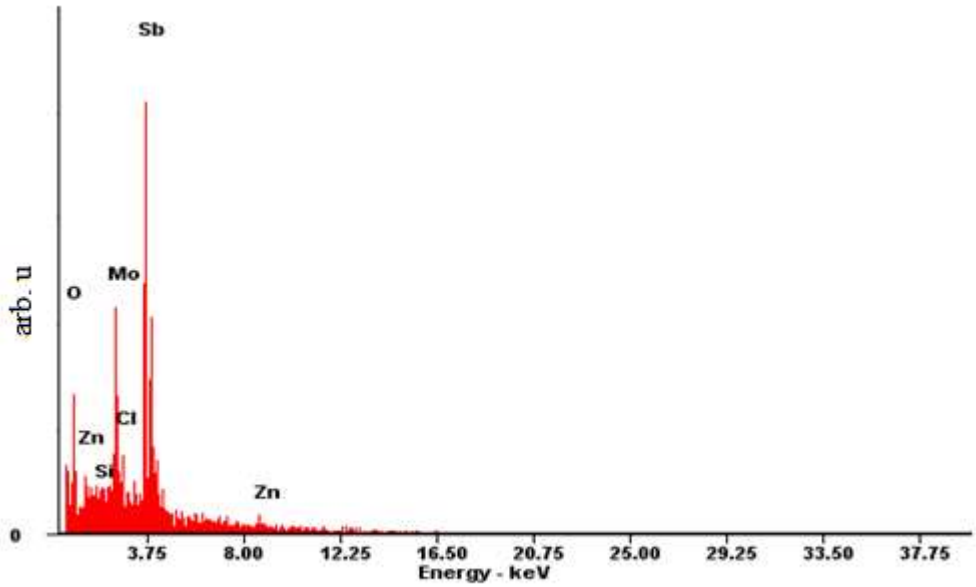


Figure 2

ACCEPTED MANUSCRIPT

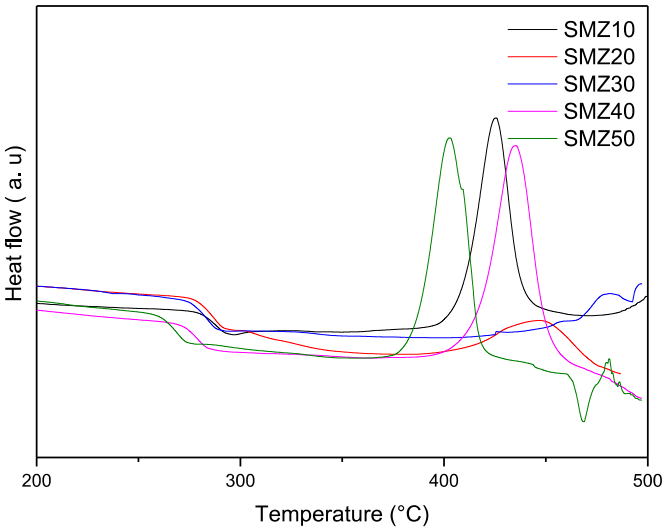


Figure 3

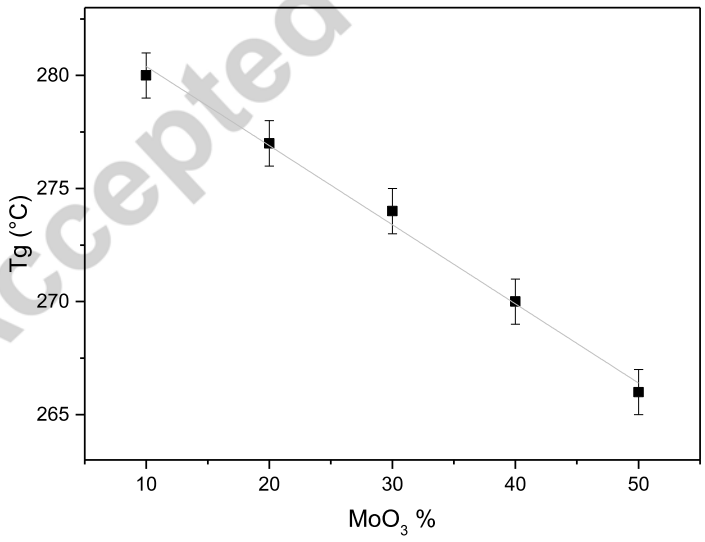


Figure 4

Accepted manuscript

ACCEPTED MANUSCRIPT

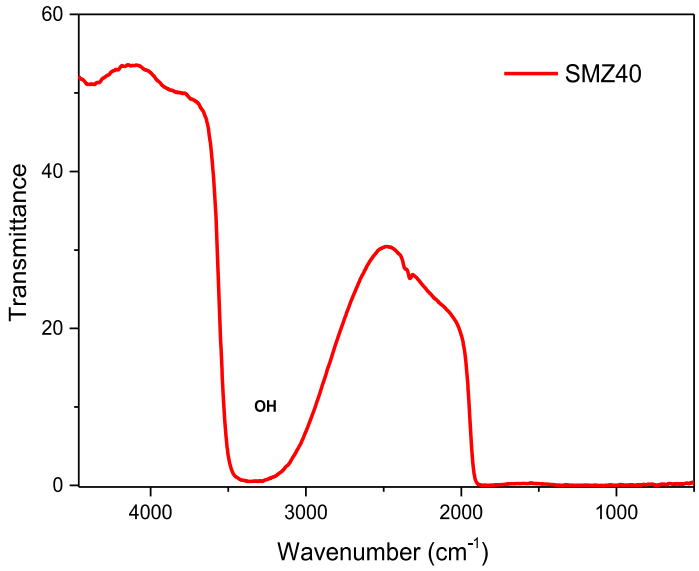


Figure 5

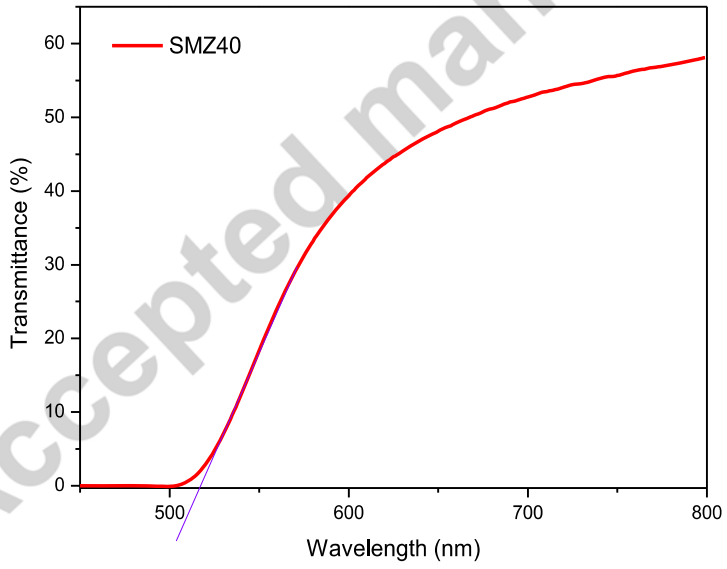


Figure 6

Accepted manuscript

ACCEPTED MANUSCRIPT

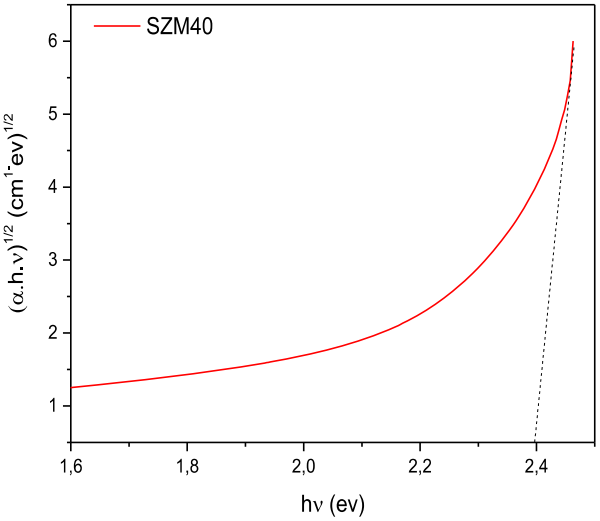


Figure 7

Accepted manuscript

ACCEPTED MANUSCRIPT

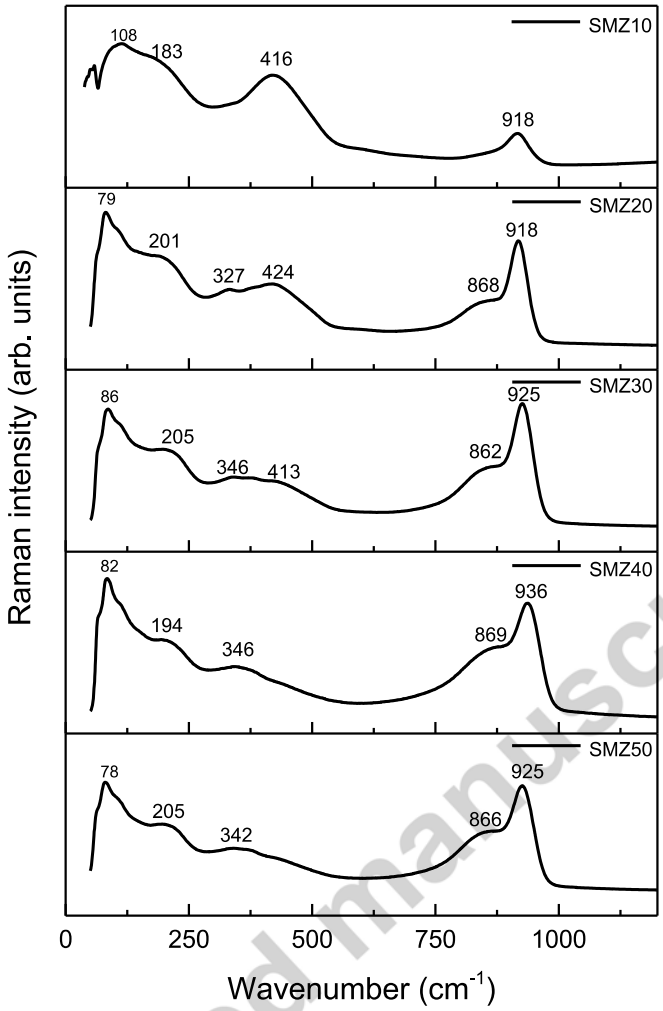


Figure 8

Accepted manuscript

ACCEPTED MANUSCRIPT

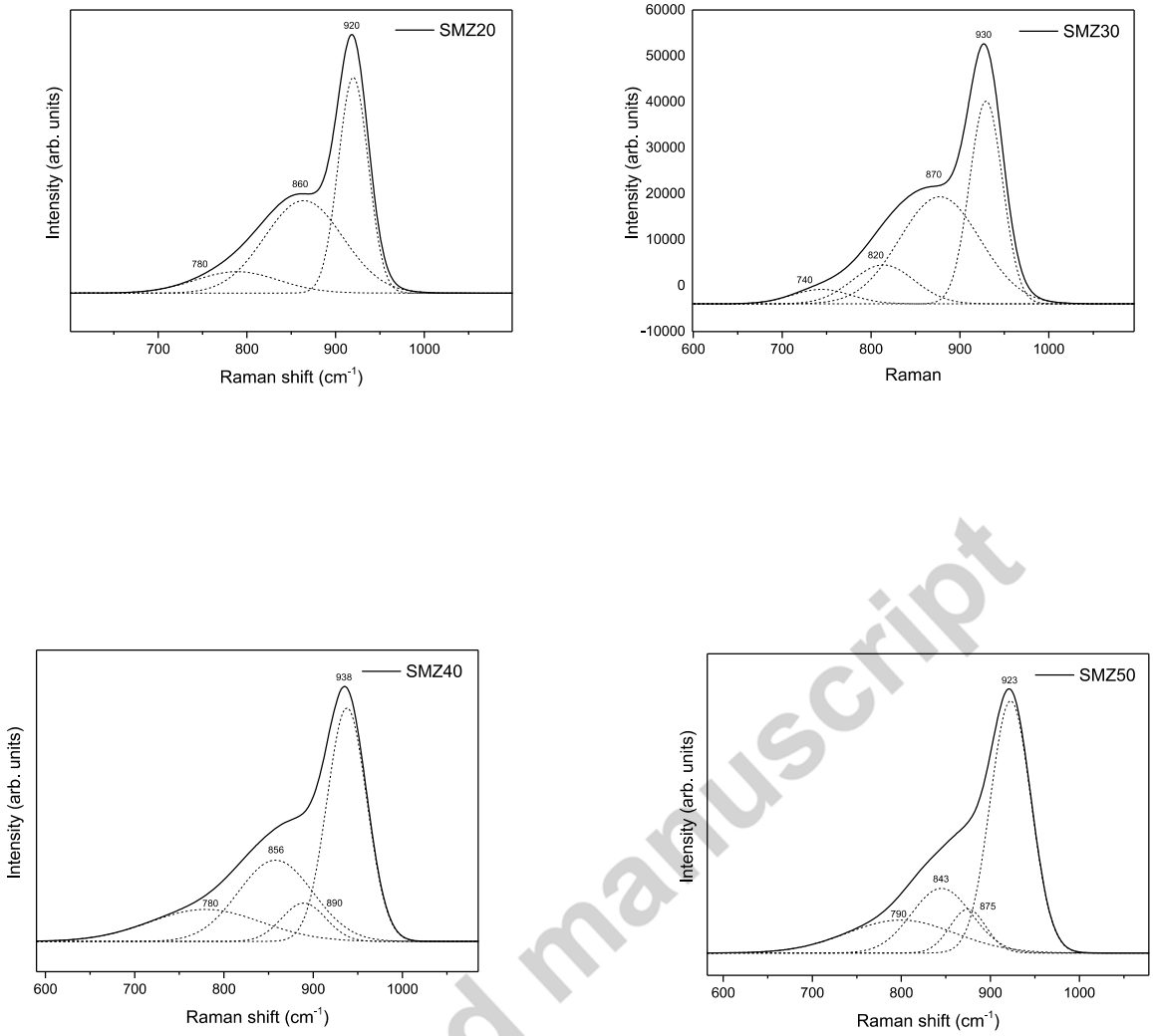


Figure 9

Accepted manuscript

ACCEPTED MANUSCRIPT

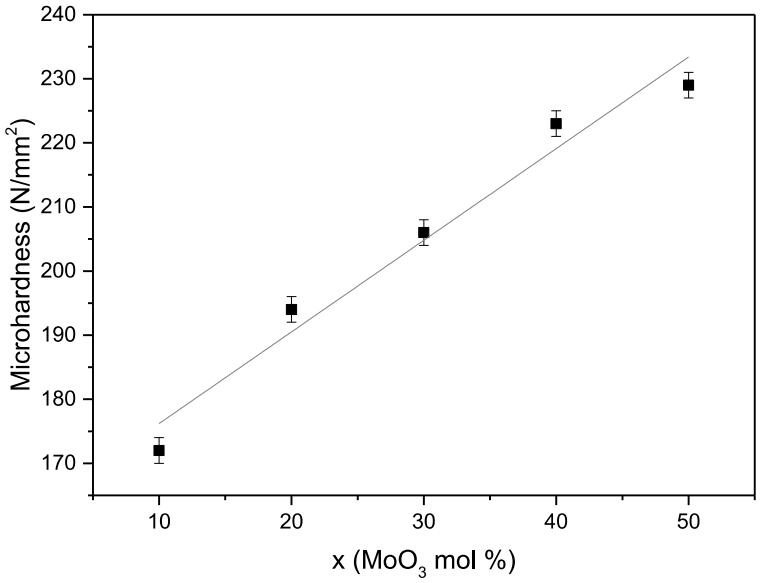


Figure 10

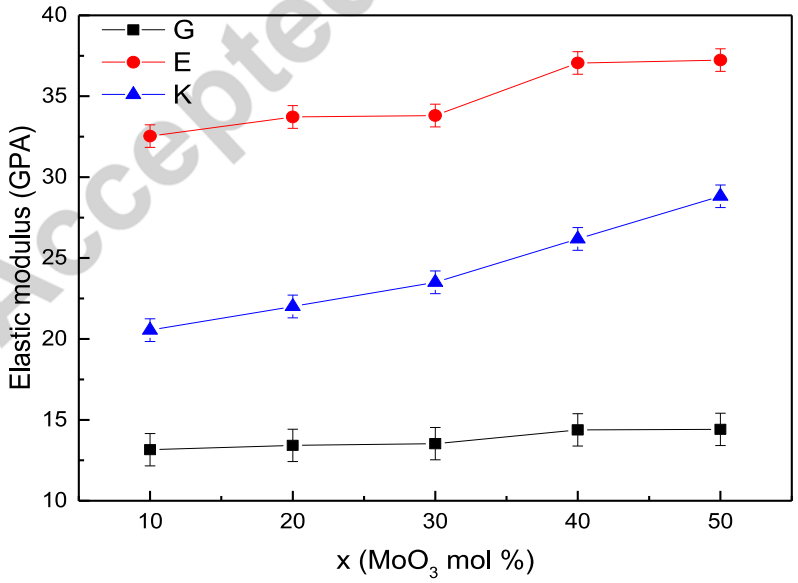


Figure 11

Accepted manuscript